Solid State Ionics 343 (2019) 115129

Contents lists available at ScienceDirect

Solid State Ionics

journal homepage: www.elsevier.com/locate/ssi

Optimization of low value electrodeposition parameters of nano-structured NiO electrochromic thin films

Iyad Saadeddin[a,*], Mohammed Suleiman[a], Haneen Salman[a], Khawla Zrikem[b], Giljoo Song[b], Aline Rougier[b]

[a] Faculty of Science, An-Najah National University, Nablus, Palestine
[b] CNRS, Univ. Bordeaux, Bordeaux INP, ICMCB, UMR 5026, F-33600 Pessac, France

ARTICLE INFO

Keywords:
Nickel oxide
Electrodeposition parameters
Electrochromism

ABSTRACT

In this work, the electrochromic and structural properties of NiO thin films prepared using optimized low value electrodeposition parameters were studied. The optimized parameters were deposition current density, molar concentration of nickel nitrate solution, and deposited charge density. The highest electrochromic characteristics corresponded to deposition parameters of $-0.05\ mA/cm^2$ deposition current density, 0.02 M of $Ni(NO_3)_2.6H_2O$ solution, and charge density of $80\ mC/cm^2$. For this optimized film, at 630 nm wavelength, the transmittance modulation ΔT was 76%, the efficiency η was $19\ cm^2/C$, the charge reversibility Q_c/Q_a was 97%, and a remarkable contrast ratio CR of 5.9. In addition, a good cycling stability was confirmed up to 900 cycles. Optimized NiO thin films were poorly crystallized exhibiting a nano-flake structure, high porosity, and homogeneity.

1. Introduction

One of the most extensively used transition metal oxides showing semiconducting properties is Nickel oxide (NiO). This binary oxide is widely used in many applications like electrochromic devices [1,2], photo electrolysis catalyst [3], fuel cells [4], electrode in batteries [5], and supercapacitors [6]. Focusing on electrochromism, anodically colored NiO thin films reversibly switch from a transparent to a brownish state on oxidation/reduction through the Ni^{+3}/Ni^{+2} redox process [7]. NiO is often used as complementary material in commercialized WO_3 based devices considering smart windows applications for instance [8]. NiO thin films have been deposited using many techniques like sputtering [9,10], e-beam evaporation [11], thermal decomposition [12], chemical deposition reaction [13], dipping in sol–gel [2,12], spray pyrolysis [14], and electrodeposition [15–17]. Among the various chemical and physical deposition techniques, electrodeposition has received significant interest allowing large surface area at room temperature, being low cost and friendly for the environment [18]. Upon thermal treatment, electrodeposited films showed an adhesion improvement with slight increase in film capacity [19]. Enhancement of transmittance modulation and cycling stability were found for electrodeposited film doped with dopants like Ce and Cu [20,21]. Also, electrodeposited films exhibit ageing after a few cycles [19,20].

To our knowledge, up to now, studies on Ni-based electrochromic film deposited by electrodeposition technique did not investigate an optimization of electrodeposition parameters using only low values, such as low current densities, low concentration contents in the solution, or low deposited charge density.

In the present work, optimization of different electrodeposited low parameters values has been performed aiming at the deposition of efficient electrochromic nano-structured NiO thin films onto FTO/glass substrate.

2. Experimental

Electrodeposition of NiO films was carried out in hydrated nickel nitrate [$Ni(NO_3)_2.6H_2O$] (99.99% from Sigma-Aldrich) aqueous solution with low concentration ranges from 0.01–0.04 M. The depositions were done on $4 \times 1\ cm^2$ FTO/glass substrate (Sigma-Aldrich) having a sheet resistance of about 7 Ω/square. Prior to electrodeposition, the substrates were ultrasonic cleaned in isopropanol, acetone, and ethanol successively for 10 min in each solution. After that substrates were treated with diluted HCl and rinsed with deionized water.

Electrodeposition were carried out at applied low current density ranging from -0.05 to $-0.25\ mA/cm^2$ using the universal potentiostat PGZ 402 (Radiometer Analytical) via Galvanostatic Coulometry

* Corresponding author at: An-Najah National University, P. O. box: 07, Nablus, Palestine.
E-mail address: iyads@najah.edu (I. Saadeddin).

https://doi.org/10.1016/j.ssi.2019.115129
Received 26 August 2019; Received in revised form 25 September 2019; Accepted 24 October 2019

procedure. The deposition was performed in a three electrodes cell with saturated calomel electrode (SCE) used as reference electrode. The substrate was connected to working electrode and the counter electrode was attached to platinum sheet electrode. Low magnitude deposited charges, ranging from 20 to 120 mC/cm^2, were deposited on the substrates. After electrodeposition, the films were washed, dried, and then annealed at 300 °C for 1 h in order to obtain NiO thin films from electrodeposited $Ni(OH)_2$ films [22]. The same potentiostat combined with a three electrodes cell was used to perform electrochemical cyclic voltammetry (CV). CVs were measured using 0.1 M KOH as an electrolyte, with a scan rate of 50 mV/s in a potential sweeping between −200 and 800 mV at room temperature. Optical transmission spectra study was operated in situ with CV measurements using Shimadzu UV-3101PC UV-VIS-NIR Scanning Spectrophotometer. The morphology of the films was studied by Scanning Electron Microscopy (SEM) using Hitachi Tabletop microscope TM-100. The structure of the films was characterized by X-ray diffraction (XRD) using a PANanalytical X'pert MPD diffractometer with Cu-Kα incident radiation.

3. Results and discussion

In order to reach high performance electrochromic properties of NiO thin film layer, different film deposition parameters have been optimized, focusing mainly on film deposition current density (J_d), hydrated nickel nitrate molar concentration in deposition solution, and deposited charge density.

3.1. Optimization of deposition current density (J_d)

Five different current densities (−0.05, −0.10, −0.15, −0.20 and −0.25 mA/cm^2) were used for room temperature electrodeposition of NiO film on FTO/glass substrate. 0.01 M $Ni(NO_3)_2.6H_2O$ was used as the deposition solution. The deposited charge density for all films was 80 mC/cm^2. As expected, the deposition time was observed to linearly decrease with increasing J_d. The deposition time, for −0.05 mA/cm^2 current density, was 26 min and this time halved as the current density value doubled.

Electrochromic behavior of various films was tested by CV combined with optical transmittance. CV measurements were performed from −200 to 800 mV versus SCE at a scan rate of 50 mV/s in 0.1 M KOH solution. CVs of NiO film deposited at −0.05 mA/cm^2 are shown in Fig. 1.

CVs exhibit the typical shape of NiO films cycled in KOH medium [23]. Upon cycling, the current density of the anodic peak J_a and cathodic peak J_c values increase. In addition, the anodic and cathodic peak potentials (V_a and V_c) shift continuously to higher and lower potential respectively. Increasing the intensity peak values and related potential shifting indicate an increase in the amount of inserted charges

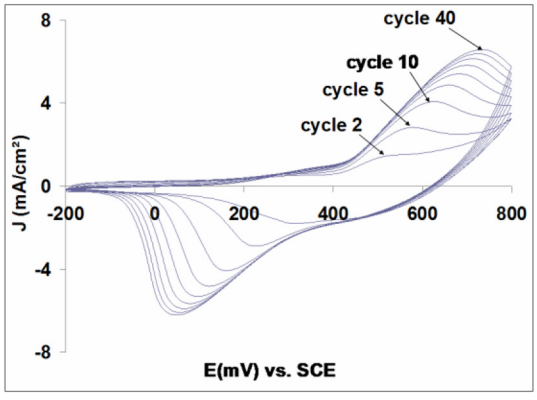

Fig. 1. 40 cycles of CV for NiO films deposited at J_d = −0.05 mA/cm^2 and cycled in a three electrodes cell, NiO/KOH (0.1 M)/Pt.

within the film layer upon Ni^{+3}/Ni^{+2} redox process. This period on early cycling is called the activation period. During this period, the increase in capacity is due to the chemical transformation of NiO to electrochemically active $Ni(OH)_2$ according to the reaction $NiO + H_2O \rightarrow Ni(OH)_2$. This reaction occurs at the NiO grains surfaces that have an intimate contact with the aqueous electrolyte solution. The activation period may vary from few to hundreds of cycles depending on many different parameters like film thickness, film structure, concentration of KOH, and applied potential [24]. Other films deposited at −0.10, −0.15, −0.20, and −0.25 mA/cm^2, adopt a similar curve behavior as shown in Fig. 2. Variations in J_a, J_c, V_a, and V_c between different curves of different J_d's (see Fig. 6) will be discussed later on in this section for cycle 40.

In situ transmittance of light through the films was recorded for 40 cycles. CV measurements and corresponding percentage transmittance [T(%)] through the film deposited at −0.05 mA/cm^2 at 630 nm are shown in Fig. 3. During the anodic and cathodic part of CV cycles, the coloration and bleaching of the film take place respectively according to the conventional reversible reaction [24,25]:

$$Ni(OH)_2 + OH^- \leftrightarrow NiOOH + H_2O + e^- \quad (1)$$

where $Ni(OH)_2$ is transparent and NiOOH adopts a brownish color.

The evolution of the transmittance during the 40 cycles of CVs for the NiO film deposited at J_d of −0.05 mA/cm^2 is presented in Fig. 4.

Fig. 4 shows a continuous decrease in the transmittance of the colored state, during cycling (The transmittance decreases from 49.8 to 13.1% for the cycles 1 to 40 respectively). This decrease is due to an increase in the coloration "sites" [$Ni(OH)_2$] involved in the coloring process during the activation period. Also, the decrease in transmittance becomes very small after 35 cycles as the cycling seems to approach the saturation period; the whole film surface that could be cycled is almost reached [24]. On the other hand, a high film transparency (transmittance > 90%) in the bleached state was observed. More precisely, on early cycling the transmittance of high value, 96.4%, progressively decreases to become essentially constant (about 90.5%) when approaching the saturation period. The decrease in transmittance in the bleached state could be assigned to unequal anodic Q_a and cathodic Q_c charge densities and unsteady charge reversibility (Q_c/Q_a is not constant) through the electrochromic layer, during the activation period. The high decrease in film coloration transparency, T_c, and small decrease in the bleaching transparency, T_b, causes an increase in light transmittance modulation ($\Delta T = T_b - T_c$). The transmittance modulation increases from 45% to 77% when cycling the film from 1 to 40 cycles. Other films deposited at −0.10, −0.15, −0.20, and −0.25 mA/cm^2, adopt a similar curve behavior as shown in Fig. 5. Comparison between different curves deposited at different J_d's (see Fig. 8) will be discussed here after in this section.

Comparing CVs of cycle 40 for films deposited at different current densities (Fig. 6) indicates an increase in J_a and V_a and a decrease in J_c and V_c with increasing J_d from −0.05 to −0.15 mA/cm^2 (see Inset a and b of Fig. 6). This corresponds to an increase in the film capacity caused by an increase of a porous surface morphology and hence an increase in the surface active sites of NiO layer (i.e. $Ni(OH)_2$ active surface) [26].

For other deposited films, a decrease in J_a and V_a and an increase in J_c and V_c was observed with increasing J_d for −0.20 and −0.25 mA/cm^2. Increasing crystallite size with increasing J_d was earlier attributed by F. Ibrahimi et al. to the evolution of more hydrogen at electrode-liquid interface when electrodepositing Ni cystallites [27]. The X-ray diffractograms show that NiO thin films are nano-crystallized in the cubic rock-salt structure (*Fm-3m*), with a major peak located at about 43° corresponding to the (200) indexation. Other observed peaks are for FTO substrate layer. The estimation of the crystallite size using the Scherrer equation, $L = 0.89\lambda = \beta \cos\theta$, where L is the average crystallite size in nm, λ = 0.154056 nm, β is the full width at the half maximum, and θ is the diffraction angle, shows an increase from about

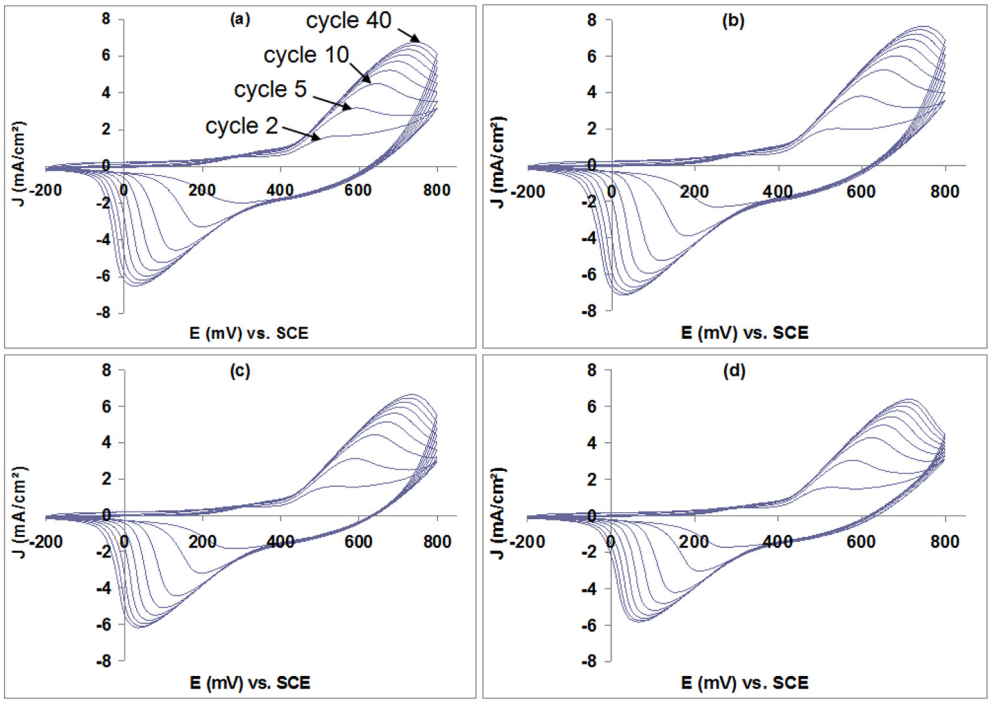

Fig. 2. 40 CV cycles for NiO films deposited at different J_d of (a) -0.1 mA/cm^2, (b) -0.15 mA/cm^2, (c) -0.20 mA/cm^2 and, (d) -0.25 mA/cm^2. All films are cycled in a three electrodes cell, NiO/KOH (0.1 M)/Pt.

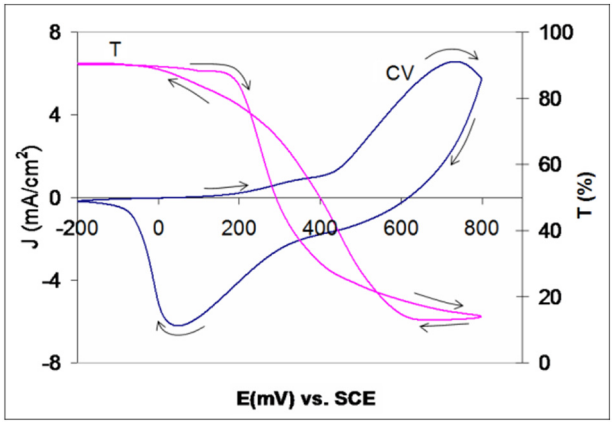

Fig. 3. Variation of transmittance T at 630 nm during CV measurements for cycle number 40 of NiO film deposited at J_d of -0.05 mA/cm^2.

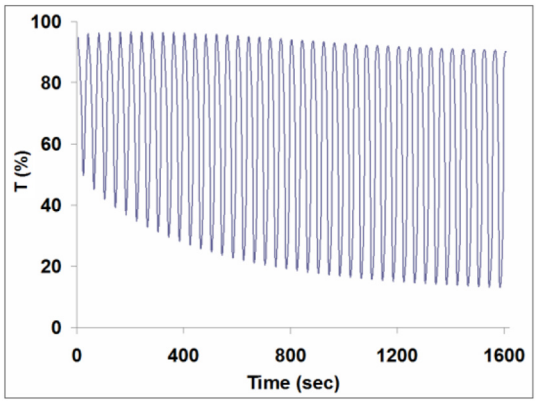

Fig. 4. Evolution of the transmittance recorded at 630 nm during 40 CV cycles for NiO film deposited at J_d of -0.05 mA/cm^2.

25 nm to 45 nm as J_d increases from -0.05 to -0.25 mA/cm^2 (Fig. 7).

The increase in the crystallite size decreases the surface active area (less $Ni(OH)_2$ conversion) and hence decrease the overall NiO film reactivity. This will indeed decrease the amount of charge insertion within the structure of the film.

The evolution of the transmittance recorded during CV measurements for the cycles 1 to 4 and 37 to 40 for all films prepared at different current densities is presented in Fig. 8. All the films show high transparency (transmittance > 90%) in the bleached state that slightly decreases when increasing cycles from 4 to 37.

All films show high transparency in the bleached state (above 90%). However, in the colored state, the "intensity" of coloration decreases (higher transmittance value) with increasing J_d. This leads to a decrease in ΔT value. Highest ΔT observed for lower J_d (-0.05 mA/cm^2). This is in agreement with previously mentioned higher surface area for less J_d due to smaller grain size.

Electrochromic properties for cycle 40 for films deposited from different current densities are calculated and presented in Table 1. Anodic and cathodic charge densities (Q_a and Q_c) into NiO films during CV were deduced from the area under current density J versus time t graphs according to the fundamental formula [23,28]:

$$Q = \int J dt \tag{2}$$

In respect of electrolyte decomposition (i.e. water oxidation), the anodic capacity is always overestimated.

The coloration efficiency η of the films were calculated using T_b and T_c, in addition to cathodic charge density Q_c, according to [23,28]:

$$\eta = \frac{\Delta OD}{Q_c} \tag{3}$$

where $\Delta OD = \log \frac{T_b}{T_c}$ is the optical density change, and T_b/T_c is called the contrast ratio (CR).

From Table 1, the highest ΔT, ΔOD, and η are observed for films deposited at deposition current density $J_d = -0.05$ mA/cm^2. In addition, this film has the highest contrast ratio CR, and a high charge reversibility of 0.92. As a result, one can consider the optimized

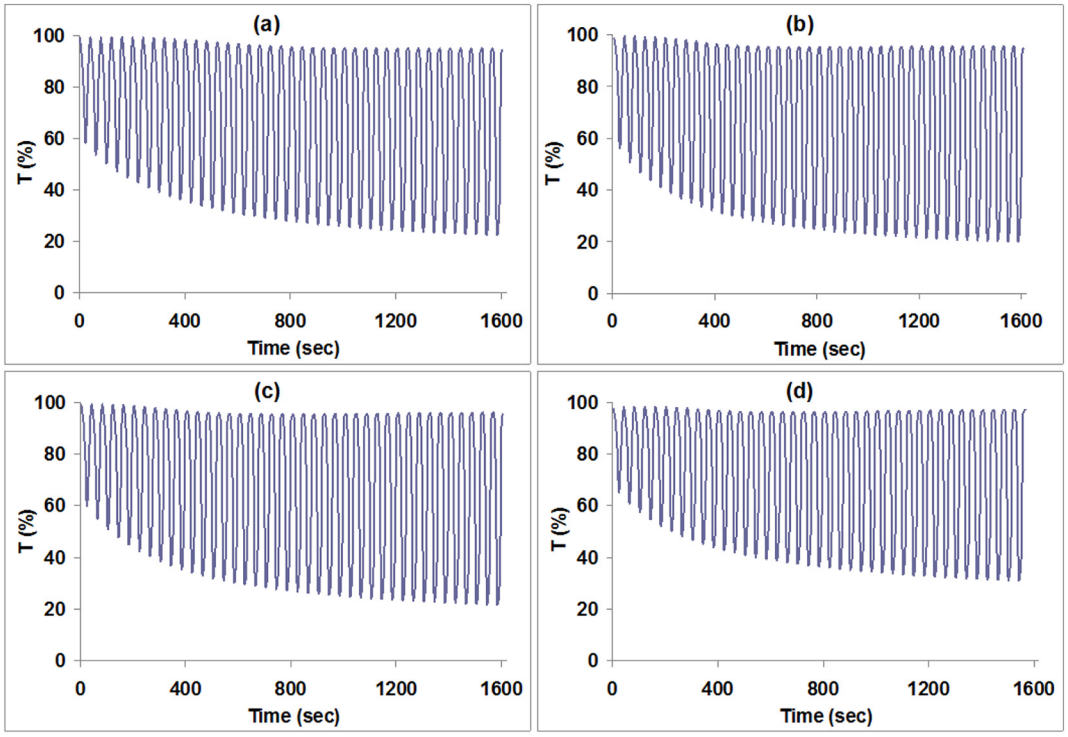

Fig. 5. Evolution of the transmittance recorded at 630 nm during 40 CV cycles for NiO films deposited at J_d of (a) −0.1 mA/cm^2, (b) −0.15 mA/cm^2, (c) −0.20 mA/cm^2 and, (d) −0.25 mA/cm^2.

electrodeposition current density for NiO films to be −0.05 mA/cm^2. This current density was chosen to further optimize other parameters that affect the electrodeposition process of NiO films.

3.2. Optimization of hydrated nickel nitrate molar concentration

NiO thin films were electrodeposited from the aqueous solution containing $Ni(NO_3)_2.6H_2O$ with different molar concentrations (0.01 M, 0.02 M, 0.03 M, 0.04 M). For all films the deposition current density used was the previously optimized J_d of −0.05 mA/cm^2 and the

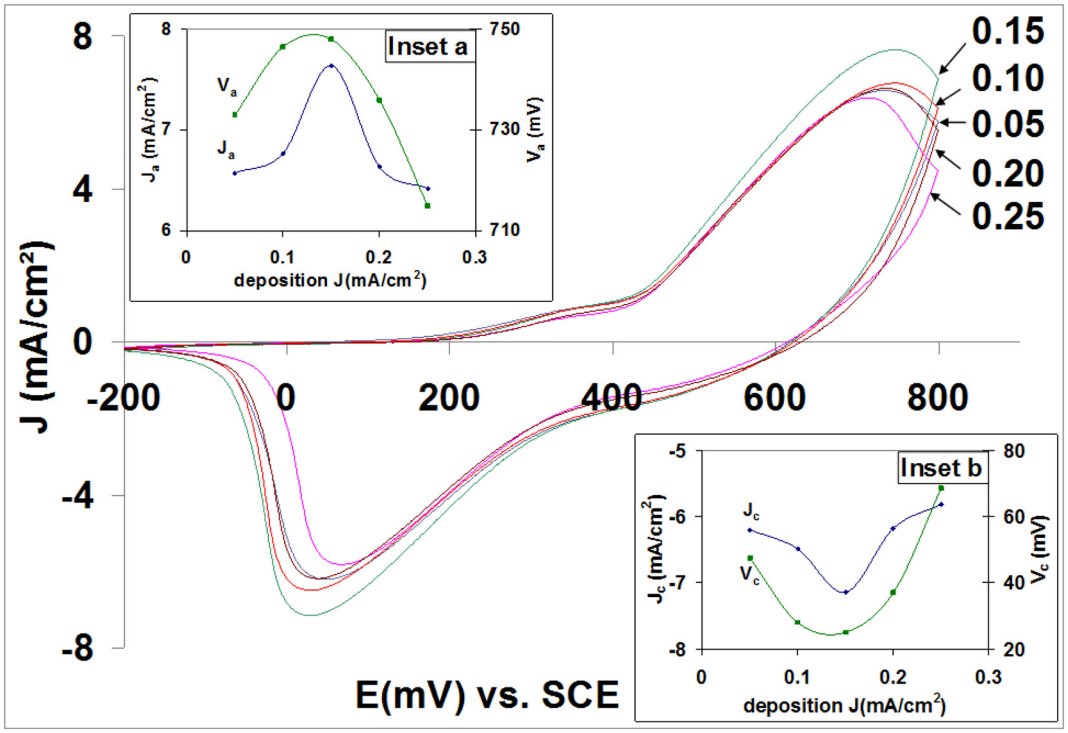

Fig. 6. CVs for cycle 40 of films deposited at different J_d (−0.05, −0.10, −0.15, −0.20, and −0.25 mA/cm^2). Inset a is I_a and V_a and inset b is I_c and V_c variations for different deposited films.

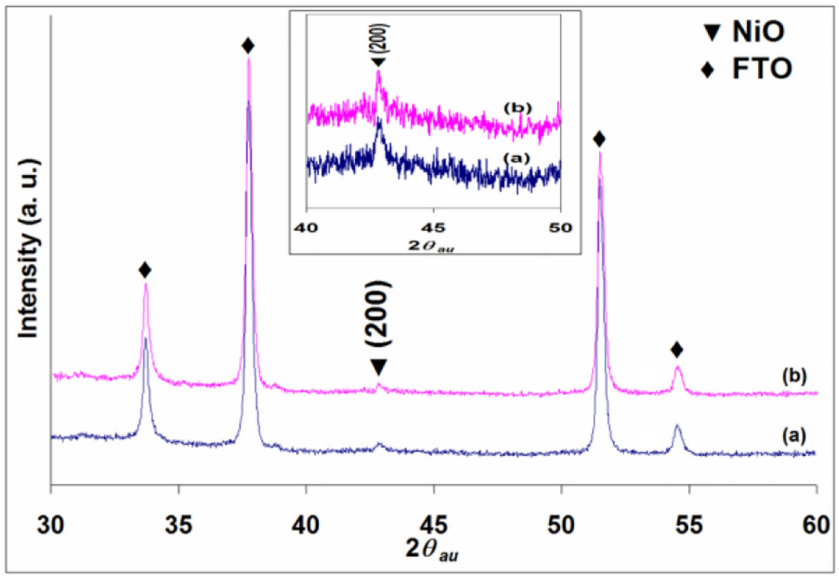

Fig. 7. X-ray diffractogram of NiO thin films deposited at (a) $-0.05\ mA/cm^2$ and (b) $-0.25\ mA/cm^2$ on FTO/glass substrate. The inset shows a magnification of (200) peak.

amount of charge deposited was constant as before ($80\ mC/cm^2$).

In order to study the electrochromic properties of the films, CV and in situ transmittance were recorded. As expected, the films show an increase in capacity during the activation period (Fig. 9a shows an example for film deposited at a concentration of 0.04 M). The corresponding coloration/bleaching light transmittance is shown in Fig. 9b. ΔT increases in the activation period and becomes almost constant near the saturation period. Same tendency was observed for other films deposited at 0.01 M, 0.02 M, and 0.03 M.

The comparison between all the films deposited at different molar concentrations indicates that the anodic peaks and cathodic peaks and their corresponding potentials (cycle 40) are close in value for films deposited at 0.01 and 0.02 M (Fig. 9c) suggesting close electrochromic properties. However, for concentrations of 0.03 and 0.04 M, the anodic and cathodic peak values decrease and shift in potential indicating a decrease in the films capacity and hence less electrochromic performances in term of coloration and bleaching of the films. Increasing the molar concentration in the solution decreases the film porosity due to a decrease in the uniformity of the electrochemical reaction [29]. The decrease in porosity of the film decreases the active surface area and hence less reaction occurs at the grain boundaries. This leads to higher transparency in the colored state (less coloration) of the film as it is clearly shown in Fig. 9d.

The light transmittance for all films deposited at different molar concentrations (Fig. 9d) was high in the bleached state (above 90%) for all recorded cycles in the active or near saturation region. In the colored state, the highest coloration was observed for film deposited at lower concentration values of 0.01 and 0.02 M. Hence these films exhibited highest ΔT. On the other hand, the transparency in the colored state was lower (less color) for films deposited at concentration of 0.03 and 0.04 M corresponding to lowest ΔT.

From the above data of different films deposited at different molar concentration solutions, electrochromic properties for cycle 40 were calculated and presented in Table 2.

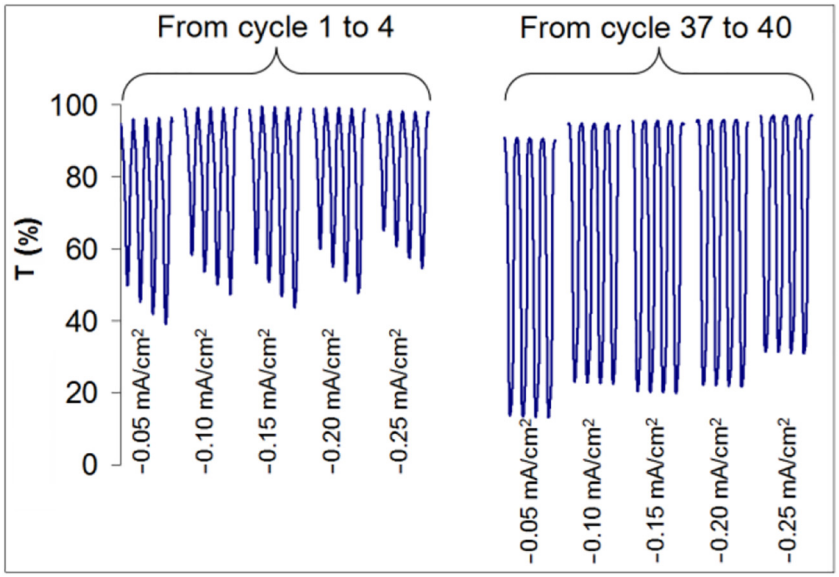

Fig. 8. Evolution of the transmittance, recorded at 630 nm, during 1 to 4 and 37 to 40 cycles for NiO films deposited at different J_d (-0.05, -0.10, -0.15, -0.20, and $-0.25\ mA/cm^2$).

Table 1
Electrochromic properties of cycle 40 for films deposited using different J_d.

J_d (mA/cm^2)	T_b ± 1.5 (%)	T_c ± 1.5 (%)	ΔT ± 3 (%)	CR ± 12%	Q_a ± 1 (mC/cm^2)	Q_c ± 1 (mC/cm^2)	η ± 1.5 (cm^2/C)	Q_c/Q_a ± 0.04
−0.05	90.7	13.1	77.6	6.9	45.0	41.5	20.2	0.92
−0.10	94.9	22.5	72.4	4.2	45.2	42.7	14.6	0.94
−0.15	95.7	19.9	75.8	4.8	50.2	47.1	14.5	0.94
−0.20	95.8	21.7	74.1	4.4	42.2	39.3	16.4	0.93
−0.25	97.1	30.9	66.2	3.1	41.00	35.2	14.1	0.86

For films deposited at 0.01 and 0.02 M, close electrochromic properties are obtained. However, the film deposited at 0.02 M is favored due to highest transmittance modulation ΔT, highest efficiency η, highest contrast ratio CR, and highest charge reversibility Q_c/Q_a. On the other hand, as expected, less capacity is observed for films deposited at 0.03 and 0.04 M. This could be observed from Q_a and Q_c recorded in Table 2, which have lower values than their counterparts deposited at 0.01 and 0.02 M. According to the obtained results measured at cycle 40, the highest electrochromic properties were observed for films deposited at $Ni(NO_3)_2.6H_2O$ concentration of 0.02 M. This molar concentration, in addition to previously optimized deposition current density (−0.05 mA/cm^2) will be considered to deposit NiO films with different charge densities (different thickness).

3.3. Optimization of deposition charge density (Q_d)

NiO thin films were electrodeposited with different charge densities (20, 40, 80, and 120 mC/cm^2), i.e. different thickness t. The electrodeposition was performed at optimized J_d of −0.05 mA/cm^2 in an optimized aqueous solution containing 0.02 M $Ni(NO_3)_2.6H_2O$.

The film thickness (gathered in Table 3) was estimated using the charge density, deposition area, NiO density, NiO atomic weight and the two dimension porosity of the film (observed in SEM measurements Fig. 13a).

As observed for previous films, J_a and J_c values increase during the activation period (Fig. 10a shows an example for film deposited with Q_d of 40 mC/cm^2). This increase is accompanied with shift to higher and lower potentials for J_a and J_c, respectively. This behavior was attributed to an increase in film capacity due to an increase in electrochemically active $Ni(OH)_2$ involved in the coloration process. Increasing capacity during the activation period will gradually increase the coloration of the film (ΔT increases) until reaching the near saturation period where the transmittance modulation ΔT becomes essentially constant. This is clearly confirmed from transmittance measurements on film deposited with Q_d of 40 mC/cm^2 (Fig. 10b). The same behavior was observed for other films of different thicknesses deposited with Q_d of 20, 80, and 120 mC/cm^2.

Comparing CV between all the films (cycle 40) of different thickness deposited at different Q_d, J_a and J_c values increase with film thickness (Fig. 10c). This is an indication of increasing active mass electrodeposited on the substrate. In addition, J_a and J_c shift to higher and lower potentials respectively. The increase in the anodic and cathodic peak current density, in addition to their shift, confirms the increase in film's capacity with increasing film's thickness. Therefore, an increase in

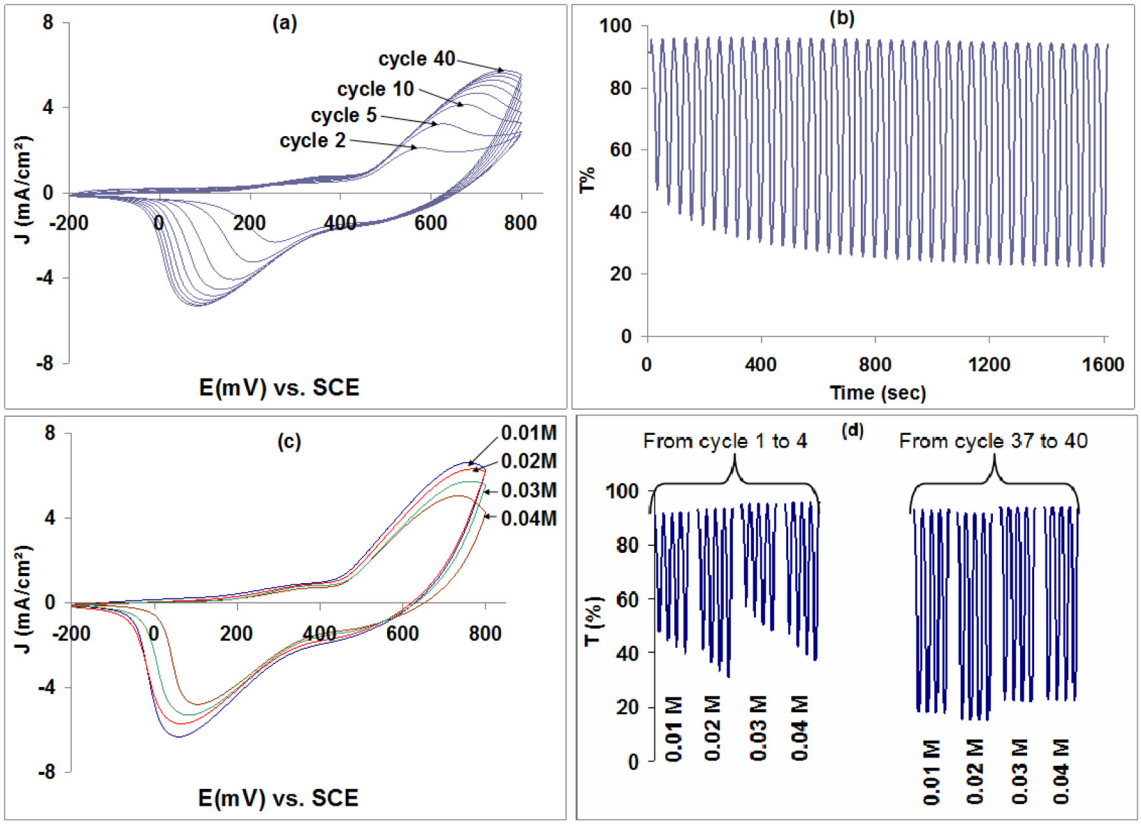

Fig. 9. CV and transmittance spectra (recorded at 630 nm) for films deposited at different molar concentrations. (a) CV for film deposited at 0.04 M, (b) Transmittance during CV for films deposited at 0.04 M, (c) CV of cycle 40 for different deposited films, and (d) transmittance in activation and near saturation regions for different deposited films.

Table 2
Electrochromic properties of cycle 40 for films deposited at different molar concentrations of $Ni(NO_3)_2.6H_2O$.

Concentration (M)	T_b ± 1.5 (%)	T_c ± 1.5 (%)	ΔT ± 3 (%)	CR ± 12%	Q_a ± 1 (mC/cm^2)	Q_c ± 1 (mC/cm^2)	η ± 1.5 (cm^2/C)	Q_c/Q_a ± 0.04
0.01	93.0	17.7	75.3	5.9	43.9	41.6	17.3	0.95
0.02	91.6	15.6	76.0	5.9	42.0	40.6	18.9	0.97
0.03	95.7	20.9	74.8	4.6	32.5	30.3	21.8	0.93
0.04	95.8	21.7	74.1	4.4	37.4	35.0	18.4	0.94

Q_a and Q_c values was observed (Table 3). Similar trends were earlier reported for NiO thin films prepared using pulsed laser deposition [24] and e-beam evaporation [11].

The transmittance of all films deposited with different Q_d (different thicknesses) in the activation and near saturation regions are shown in Fig. 10d. As expected, the transmittance of the films decrease in both bleached and colored states with increasing film thickness (The effect is more pronounced in the colored state). The decrease in transmittance with film thickness is due to larger number of grains in thicker films and hence larger scattering centers at the grain boundaries. The transparency of the films deposited with Q_d of 20, 40, and 80 mC/cm^2 in the bleached state remains high (> 93%) even when reaching the near film's saturation region. For film deposited with Q_d of 120 mC/cm^2, much lower transmittance (about 80%) was recorded in comparison to other films. In the colored state, the transmittance of films deposited with 20 and 40 mC/cm^2 remains high (less colored) as compared to other films. This may be due to a quantity of deposited material that remains lower than the amount needed for efficient electrochromic performance during the cycling of the films.

CV and transmittance data are used to deduce electrochromic properties (Table 3) for cycle 40 of the films deposited with different Q_d.

From Table 3, the film deposited with Q_d of 80 mC/cm^2 shows the highest ΔT, highest efficiency η, highest charge reversibility Q_c/Q_a, and high contrast ratio CR. Although the film deposited with Q_d of 120 mC/cm^2 have higher CR and same charge reversibility, it has lower transparency in the bleached state preventing from efficient electrochromism. Hence, the optimized Q_d for NiO film with highest electrochromic performance is 80 mC/cm^2.

4. NiO film deposited at optimized parameters

Combining parameter optimization for different low values of deposition parameters (deposition current density, molar concentration, and deposited charge density), the film showing the best electrochromic features, in term of transmittance modulation, contrast ratio, efficiency η, and charge reversibility, is the one that was deposited at a current density, J_d, of −0.05 mA/cm^2 using 0.02 M $Ni(NO_3)_2.6H_2O$ aqueous solution with deposition charge density, Q_d, of 80 mC/cm^2.

For the optimized electrochromic film, different parameters and properties were further investigated in terms of electrochromic activity, cycling stability, optical modulation, surface morphology and structure.

4.1. Electrochromic properties

As described above for all films, CVs for optimized NiO film (Fig. 11a) show an increase in J_a and J_c with shifting to higher and lower values in their potential, respectively. This indicates (as previously quoted) that the film capacity increases with increasing cycle number during the activation period [24]. The increase in capacity is related to an increase in $Ni(OH)_2$ amount involved in the coloration process of NiO at the grain boundary. Hence an increase in the surface area exposed to coloration/bleaching reaction. As a result of increasing film capacity, the amount of charge density inserted during coloration (Q_a) and bleaching (Q_c) increases as shown in Fig. 11b. The difference between Q_a and Q_c is observed to decrease (Q_c/Q_a increases) with increasing cycle number and becomes almost constant near cycle 40. Charge reversibility Q_c/Q_a reaches 97% at cycle 40 (near saturation period).

The evolution of the in-situ transmittance during cycling is shown in Fig. 11c. During the activation period, the transmittance rapidly decreases with cycle number in the colored state. This trend results from an increase in the charge magnitude during coloration process due to the increase of NiO conversion into $Ni(OH)_2$. As expected, when the charge value (i.e. capacity) becomes very close to saturation, the transmittance in the colored state becomes almost constant, reaching a low value of 16.6%. In the bleached state, the film shows a high transparency (> 91%) for all the recorded 40 cycles. The decrease in transmittance in the colored state and the almost constant transmittance in the bleached state allows the transmittance modulation ΔT and contrast ratio CR to increase with increasing cycle number as clearly shown in Fig. 11d. ΔT and CR increase rapidly in the activation period and they become almost constant near the saturation period. The highest ΔT value of 76.3% and CR of 5.9 are reached near the saturation period at cycle 40.

Cycling stability of the film was examined during 900 cycles (Fig. 12) in the wavelength range 340–800 nm. As expected, the transmittance in the colored state is much lower than the transmittance in the bleached state. In the bleached state, the high transparency is linked to NiO and/or $Ni(OH)_2$ with wide energy gap of about 3.5 eV and/or 3 eV respectively [30,31]. However, for the colored state, the film structure is NiOOH with energy gap of about 1.7 eV [7]. Hence absorption of the film in the colored state for incident photons is higher and consequently lower transmittance is observed. Also the transmittance of the films is noticed to continuously increases with increasing wavelength of incident light. The increase in film transparency with increasing wavelength is higher for lower band gap NiOOH film's colored states. This was expected because as the energy of the incident light decreases, the absorption of the film decreases and hence the transmittance increases. Indeed, the higher increase in transmittance of the colored state leads to a decrease in ΔT with increasing wavelength and hence a decrease in η and CR.

Considering cycling of the film, the transmittance in the visible range initially increases in the bleached state to high values during the

Table 3
Electrochromic properties of cycle 40 for films deposited with different charge densities (Q_d).

Q_d (mC/cm^2)	t ± 4% (nm)	T_b ± 1.5 (%)	T_c ± 1.5 (%)	ΔT ± 3 (%)	CR ± 12%	Q_a ± 1 (mC/cm^2)	Q_c ± 1 (mC/cm^2)	η ± 1.5 (cm^2/C)	Q_c/Q_a ± 0.04
20	63	99.0	50.8	48.2	2.0	23.1	19.0	15.3	0.83
40	125	95.6	30.1	65.5	3.2	36.4	34.1	14.7	0.94
80	251	93.7	17.2	76.5	5.5	42.9	41.4	17.8	0.97
120	376	79.5	12.3	67.2	6.4	51.8	50.4	16.1	0.97

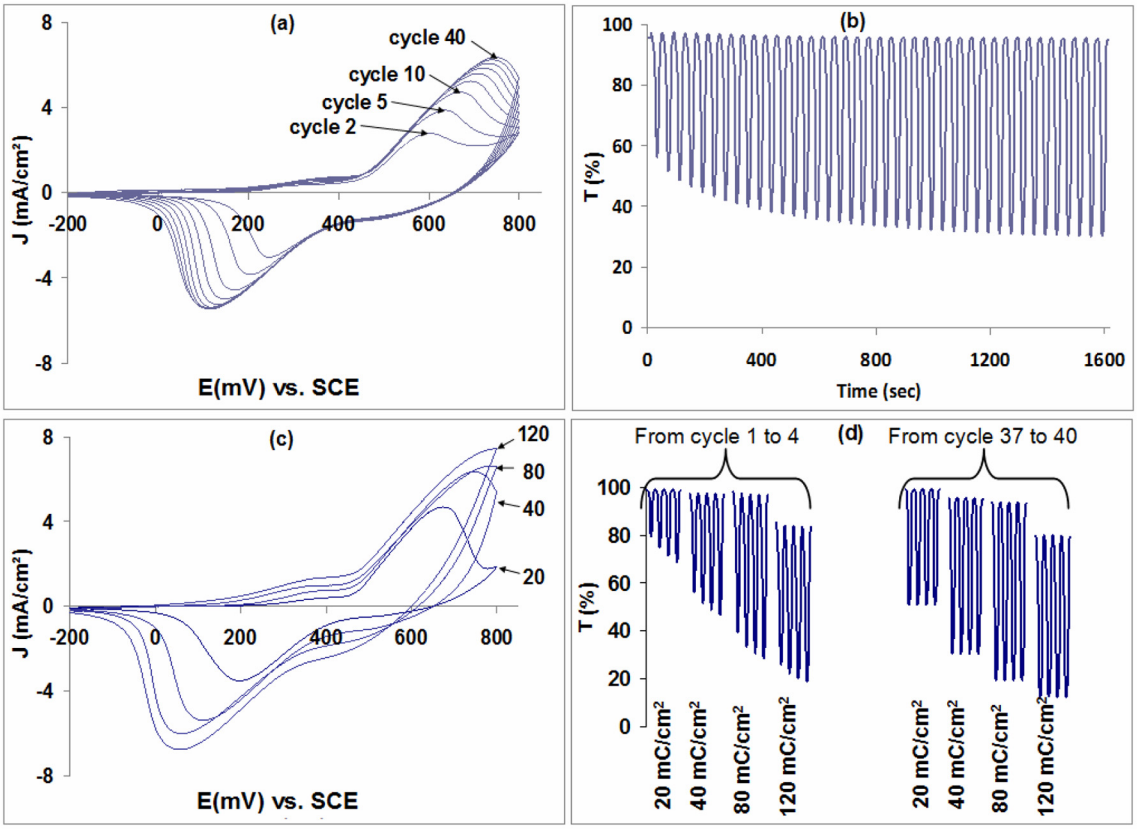

Fig. 10. CV and transmittance spectra, recorded at 630 nm, for films deposited with different charge densities: (a) CV for film deposited with 40 mC/cm^2, (b) Evolution of the transmittance during CV for films deposited with 40 mC/cm^2, (c) CV of cycle 40 for films deposited with different Q_d (20, 40, 80, and 120 mC/cm^2), and (d) transmittance in activation and near saturation regions for films deposited with different Q_d.

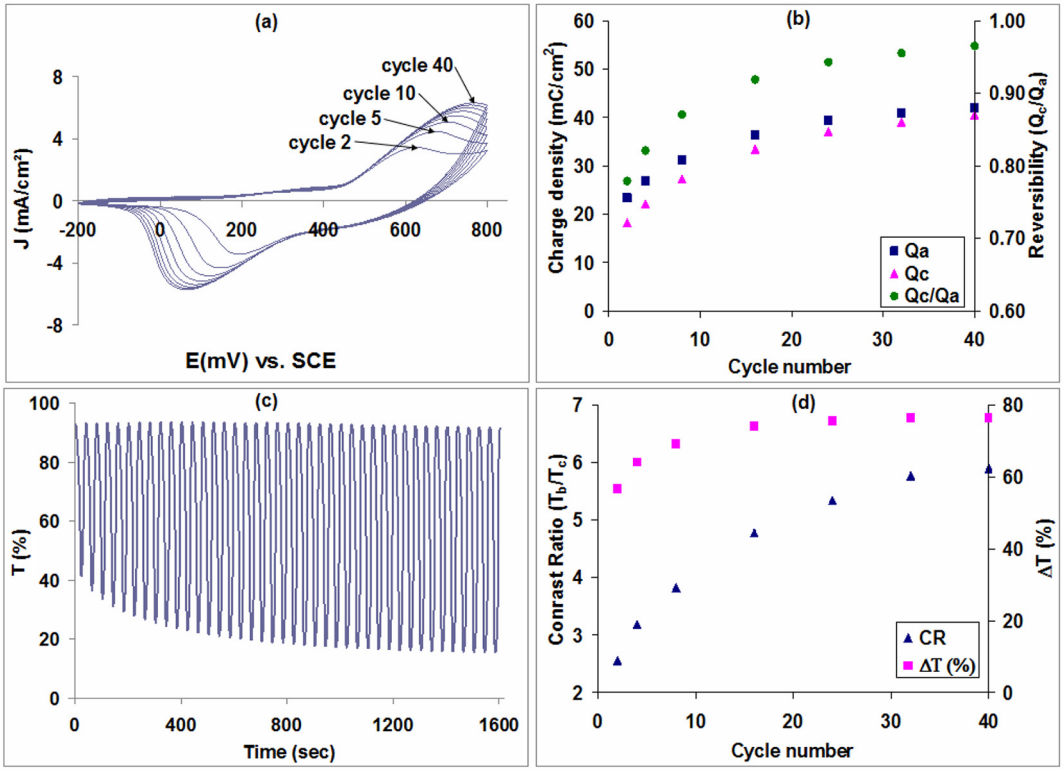

Fig. 11. Electrochromic properties of optimized NiO film: a) 40 CV cycles, b) charge densities with corresponding reversibility, c) Transmittance during CV, and d) Transmittance modulation and corresponding contrast ratio.

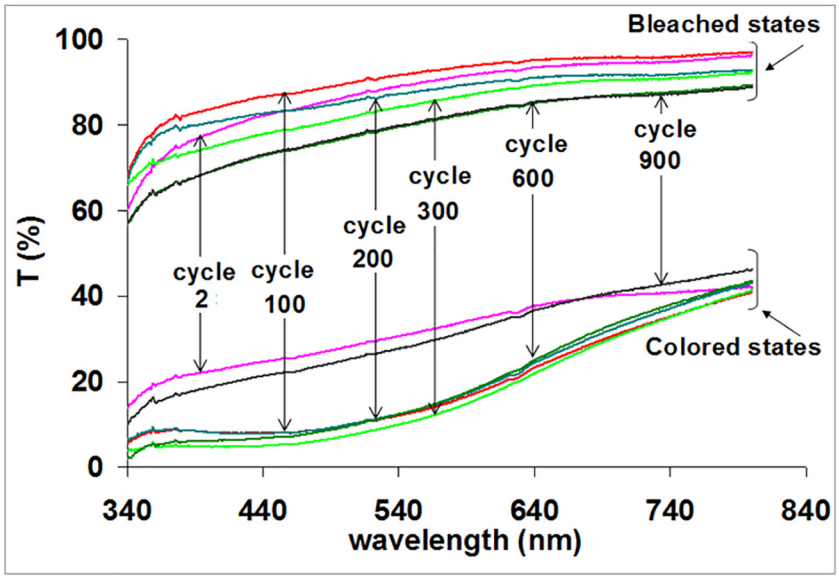

Fig. 12. Transmittance through NiO optimized film during cycling in the wavelength range of 340–800 nm.

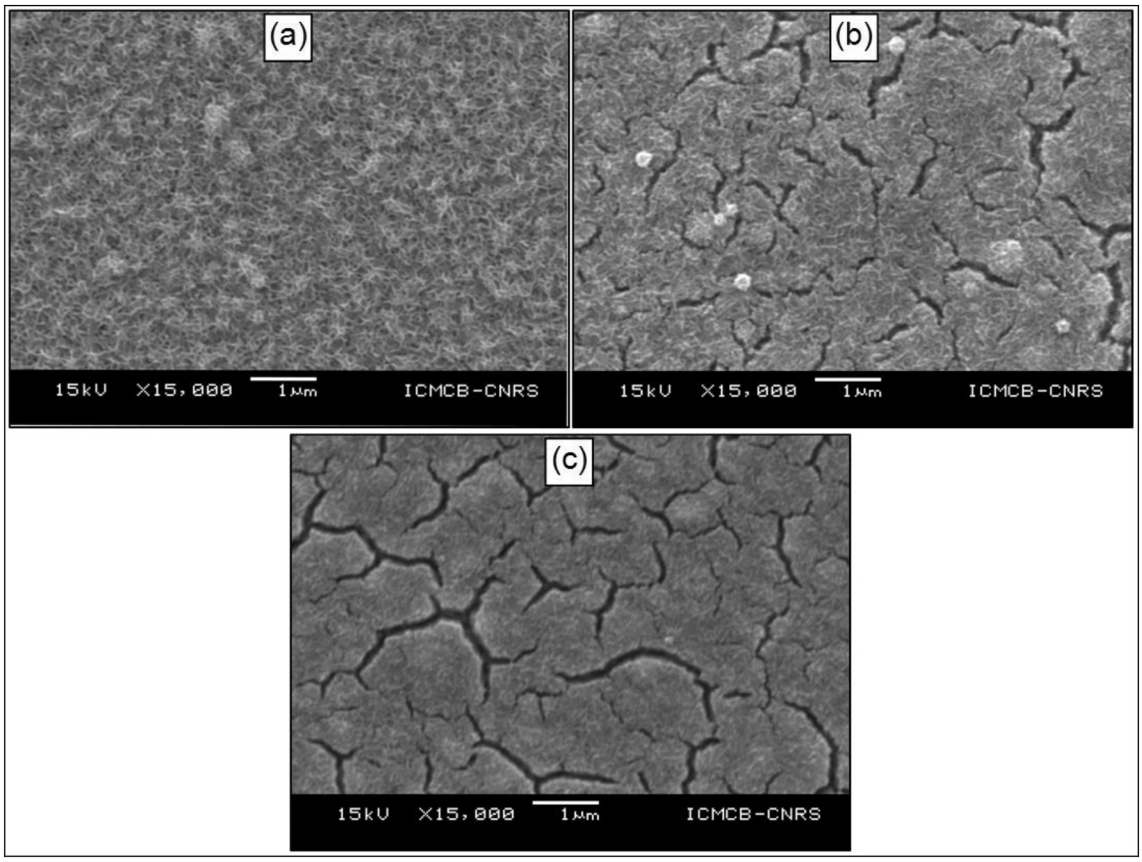

Fig. 13. SEM images for NiO films deposited at (a) optimized parameters, (b) 0.01 M aqueous solution, and (c) $-0.15\,mA/cm^2$ current density.

first 100 cycles (Fig. 12). On the other hand, the transmittance of the corresponding (first 100 cycles) colored state decreases to very low value. As earlier stated, this behavior is described increasing capacity of the film during activation period due the increase in the active sites sharing the coloration process. During cycling from 100 to 600, the transmittance decreases of about an average value of 4% for each 100 cycles, while the transmittance in the colored state almost remains constant. On the other hand, the transmittance in the colored state (less coloration) increases with an average value of 12% in the cycle range of 600–900. This could be an indicator that the film is still in the saturation region. It is worth to mention that no peeling off of the film was observed indicating that the degradation period is not reached yet.

The higher EC performance of the optimized films may be nested in the film structure or morphology.

4.2. Morphological study

Fig. 13a shows a SEM image of NiO thin film deposited in optimized

conditions, mainly deposited at $-0.05\,mA/cm^2$ with $80\,mC/cm^2$ in a solution containing 0.02 M of $Ni(NO_3)_2.6H_2O$. Fig. 13 shows nano-flakes interconnected network with pore diameter of about 50–150 nm. The surface is homogeneous without any cracks. On the other hand, changing at least one deposition parameter leads to a pronounced change in film morphology as shown in Fig. 13b and c. Film deposited using 0.01 M aqueous solution (Fig. 13b) shows more compact nano-flake structure with less pores and many cracks. Moreover, film deposited at a current density of $-0.15\,mA/cm^2$ (Fig. 13c) shows more and more compactness in the nano-flakes in addition of increasing the number of cracks in the given range of measurements. This indicates that the optimized film exhibits higher porosity and uniformity than films deposited using other deposition parameters. The high homogeneous nano-porosity observed in the nano-structured optimized film implies that the accessible surface area is greater than other films. This provides better path for electrolyte to penetrate through the film layer and hence improve the electrochromic performance.

5. Conclusion

Nickel oxide thin films were electrodeposited at low value electrodeposition parameters. The parameters investigated are deposition current density, hydrated nickel nitrate molar concentration in the deposition aqueous solution, and finally the deposited charge density in the film. Decreasing deposition current density increases the surface area of the film due to lower grain size, higher porosity and homogeneity of the film. Hence, higher electrochromic performance was recorded. The optimized deposition current density was $-0.05\,mA/cm^2$. On the other hand, film deposited at different molar concentrations showed close electrochromic properties with a 0.02 M optimized molar concentration of $Ni(NO_3)_2.6H_2O$. Moreover, increasing the film thickness, by increasing the deposited charge density, decreases the transparency of the film in both bleached and colored states, which was attributed to the increase of light scattering centers in the film. Lowest thickness thin films showed high reduction in coloration of the films colored state. In contrary, highest thickness film showed high reduction of transparency in the bleached state. Hence, the optimized film corresponds to a compromise with a film that has intermediate deposited charge density of $80\,mC/cm^2$ with estimated film thickness of 251 nm. Moreover, good cycling durability up 900 cycles was confirmed.

Acknowledgement

The authors would like to acknowledge An-Najah National University and Palestinian Ministry of Higher Education for supporting this research numbered [ANNU-MoHE-1819-Sc008].

References

[1] E. Avendano, L. Berggren, G.A. Niklasson, C.G. Granqvist, Thin Solid Films 496 (2006) 30–36.
[2] K.K. Purushothaman, G. Muralidharan, J. Sol-Gel Sci. Technol. 46 (2008) 190–194.
[3] H. Kamel, E.K. Elmaghraby, S.A. Ali, K. Abdel-Hady, Thin Solid Films 483 (2005) 330–339.
[4] N. Shaigan, D.G. Ivey, W. Chen, J. Electrochem. Soc. 155 (4) (2008) D278–D284.
[5] C.M. Lambert, G. Nazri, P.C. Yu, Sol. Energ. Mater. 16 (1987) 1–86.
[6] A. Roy, A. Ray, S. Saha, M. Ghosh, B. Satpati, M. Nandi, S. Das, T. Das, Electrochim. Acta 283 (2018) 327–337.
[7] C.G. Granqvist, Handbook of Inorganic Electrochromic Materials, Elsevier, Amsterdam, 1995.
[8] M. Da Rocha, H. Yingchun, X. Diao, A. Rougier, Sol. Energ. Mat. Sol. C. 177 (2018) 57–65.
[9] K.S. Usha, R. Sivakumar, C. Sanjeeviraja, V. Sathe, V. Ganesan, T.Y. Wange, RSC Adv. 6 (2016) 79668–79680.
[10] R.T. Wen, G.A. Niklasson, C.G. Granqvist, Thin Solid Films 565 (2014) 128–135.
[11] D.R. Sahu, T.J. Wu, S.C. Wang, J.L. Huang, J. Sci. Adv. Mater. Dev. 2 (2017) 225–232.
[12] R. Cerc Korosec, P. Bukovec, Acta Chim. Slov. 53 (2006) 136–147.
[13] X. Hou, J. Williams, K.L. Choy, Thin Solid Films 495 (2006) 262–265.
[14] D. Perednis, L.J. Gauckler, Solid State Ionics 166 (2004) 229–239.
[15] M.S. Wu, Y.A. Huang, C.H. Yang, J. Electrochem. Soc. 155 (2008) A798–A805.
[16] M.P. Browne, H. Nolan, N.C. Berner, G.S. Duesberg, P.E. Colavita, M.E.G. Lyons, Int. J. Electrochem. Sci. 11 (2016) 6636–6647.
[17] F. Vera, R. Schrebler, E. Munoz, C. Suarez, P. Cury, H. Goimez, R. Coirdova, R.E. Marotti, E.A. Dalchiele, Thin Solid Films 490 (2005) 182–188.
[18] A.I. Inamdar, S.H. Mujawar, V. Ganesan, P.S. Patil, Nanotechnology 19 (2008) 325706–325713.
[19] S. Morisaki, K. Kawakami, N. Baba, Jpn. J. Appl. Phys. 27 (1988) 314–318.
[20] D.A. Corrigan, R.M. Bendert, J. Electrochem. Soc. 136 (1989) 723–728.
[21] Y.E. Firat, A. Peksoz, Electrochim. Acta 295 (2019) 645–654.
[22] M. El-Kemary, N. Nagy, I. El-Mehasseb, Mat. Sci. Semicon. Proc. 16 (2013) 1747–1752.
[23] X.H. Xia, J.P. Tu, J. Zhang, X.L. Wang, W.K. Zhang, H. Huang, Sol. Energ. Mat. Sol. C. 92 (2008) 628–633.
[24] I. Bouessay, A. Rougier, J.M. Tarascon, J. Electrochem. Soc. 151 (6) (2004) H145–H152.
[25] G.A. Niklasson, C.G. Granqvist, J. Mater. Chem. 17 (2007) 127–156.
[26] K.W. Nam, K.B. Kim, J. Electrochem. Soc. 149 (3) (2002) A346–A354.
[27] F. Ebrahimi, Z. Ahmed, J. Appl. Electrochem. 33 (2003) 733–739.
[28] D. Rosseinsky, R.J. Mortimer, P.M.S. Monk, Electrochromism and Electrochromic Devices, Cambridge University Press, New York, 2007.
[29] C.C. Streinz, S. Matupally, J.W. Weidner, J. Electrochem. Soc. 142 (12) (1995) 4051–4056.
[30] D.R. Sahu, T.J. Wu, S.C. Wang, J.L. Huang, J. Sci. Adv. Mater. Dev. 2 (2017) 225–232.
[31] P. Hermet, L. Gourrier, J.L. Bantignies, D. Ravot, T. Michel, S. Deabate, P. Boulet, F. Henn, Phys. Rev. B 84 (2011) 235211.